A broadband and high throughput single-monochromator Raman spectrometer: Application for single-wall carbon nanotubes

Gábor Fábián,[1] Christian Kramberger,[2] Alexander Friedrich,[2] Ferenc Simon,[1,2,a] and Thomas Pichler[2]

[1]*Department of Physics, Budapest University of Technology and Economics, Budafoki út 8., Budapest, H-1111, Hungary*
[2]*Faculty of Physics, University of Vienna, Strudlhofgasse 4., Vienna, A-1090, Austria*

We present a high sensitivity single-monochromator Raman spectrometer which allows operation with a tunable laser source. The instrument is based on the modification of a commercial Raman spectrometer; such instruments operate with interference Rayleigh filters which also act as laser mirrors and are usually considered as inherently narrow band. In our design, the two tasks are separated and the filter can be freely rotated without much effect on the light alignment. Since rotation shifts the filter passband, this modification allows tunable operation with efficient stray light filtering down to 150 cm^{-1}. The design is optimized for single-wall carbon nanotubes, for which the performance is demonstrated using a tunable dye laser source. The spectrometer thus combines the high sensitivity with the broadband characteristics of usual triple monochromator systems. © *2011 American Institute of Physics*. [doi:10.1063/1.3544023]

I. INTRODUCTION

Raman spectroscopy is an important tool in various fields of science from biology to physics or even mineralogy. In particular, Raman spectroscopy became the most useful method in the fundamental studies and characterization of single-wall carbon nanotubes (SWCNTs) (Ref. [1]). The success of this method for this system and the increased demand for versatile spectrometers led to a boom in instrument development.

Raman spectroscopy is an inelastic light scattering method, where the energy transfer to and from the system is characteristic to electronic, optical, vibrational, or even magnetic properties. The method operates with monochromatic lasers as excitation. Spectrometers which can be used with a tunable laser source are referred to as "broadband" herein. The Raman spectrum consists of the intensity of the scattered photons (or Raman intensity) at a given energy transfer (also called the Raman shift).

In the special case of the so-called resonance Raman spectroscopy (RRS), the Raman intensity is enhanced when either the exciting laser or the scattered light energy matches that of an optical transition of the system. For instance, RRS enabled to increase sensitivity in heavily diluted organic compounds,[2] to distinguish between different species in minerals,[3] and to selectively enhance phonon modes with particular symmetries.[4] SWCNTs possess different transition energies depending on their diameter, therefore a laser energy dependent RRS measurement allows to identify and study SWCNTs of different kinds.

The major challenge of Raman spectroscopy is the efficient suppression of photons with wavelengths close to that of the exciting laser.[5] Such photons originate from quasielastic light scattering processes such as, e.g., Rayleigh scattering and their intensity dominates over the Raman process by a few orders of magnitude. This quasielastically scattered light is often referred to as "stray light" or "Rayleigh scattered light."

The efficient stray light suppression is particularly important for SWCNTs due to the low energy ($\geq 100-150\,\text{cm}^{-1}$) (Ref. [6]) Raman modes. This combined with the narrow (FWHM $\sim 30\,\text{meV}$) optical transition energies[7] require a broadband spectrometer with efficient stray light rejection.

Modern Raman spectrometers which allow operation down to 100 cm^{-1} contain interference Rayleigh filters rather than the classical subtractive double monochromator system. Such spectrometers are often referred to as *notch-filter* Raman systems. The principal advantage of this development is the higher signal sensitivity as typical transmission for the interference filters is above 80% for the passband, whereas transmission for the double monochromator system is significantly lower for the frequency filtered light.

A principal drawback of Raman systems with interference filters is their potentially narrow-band characteristics. This is due to the fact that interference filters are manufactured for the most common laser lines only, e.g., for those of the Ar/Kr and He/Ne lasers. In principle, the range of filter operation could be extended by rotating them. However for most spectrometers, the interference filter has a double role: it reflects the laser light to the sample and it functions as a Rayleigh filter. A rotated filter leads to a change in the optical path for the excitation that can be corrected for with a tedious spectrometer readjustment only. This is not practical for a measurement when operation with several laser lines is required. Then, what is gained by the higher sensitivity is lost upon the time spent with the readjustment.

---

a)Author to whom correspondence should be addressed. Electronic mail: ferenc.simon@univie.ac.at.

Herein, we describe the modification of a commercial Raman spectrometer with interference Rayleigh filters, which enable broadband operation with relative ease. The improvement is based on replacing the filter with a beam splitter which guides the laser light to the sample and transmits the emitted Raman light toward the spectrometer. The interference filter is inserted into the path of the backscattered light behind the beam splitter where it is rotated without affecting the excitation. Thus the double role of the interference filter is split into these two components and the rotation of the filter does not observably influence the direction of the transmitted light. Rotation of the interference filter influences the passband differently for the *S* and *P* polarizations[8] which is overcome by applying polarization filters on the spectrometer input. The setup operates with polarizations which are optimized when the so-called antenna effect of SWCNTs is taken into account, i.e., the Raman light is polarized preferentially along the polarization of the excitation.[9,10]

II. SPECTROMETER SETUP

Commercial Raman spectrometers are usually equipped with a built-in laser and a setup optimized for this single laser line; however, the characterization of SWCNTs requires measurements with a large number of laser lines[11] or with a tunable laser system.[7,12] Such a high sensitivity, confocal single monochromator Raman system with a interference Rayleigh filter can be modified to enable broadband measurements with a tunable laser, which we demonstrate for a LabRAM commercial spectrometer (Horiba Jobin-Yvon Inc.) as an example. The key step in achieving the broadband operation was replacing the built-in interference filter, which acts as a beam splitter and a Rayleigh filter at the same time, with a combination of a simple beam splitter and the separated interference filter. We note herein that this modification also enables a cost effective operation with usual laser wavelengths (such as, e.g., the lines of an Ar/Kr laser) since no complicated filter realignments are required.

The block diagram of the broadband spectrometer is shown in Fig. 1. The tunable excitation light source is a dye laser (Coherent Inc., CR-590) operated in the 545–660 nm range with a vertical polarization. Pumping is provided by a 532 nm 5 W solid state laser (Coherent Inc., Verdi G5). Three dyes, Rhodamin 110, Rhodamin 6G, and DCM (4-dicyanomethylene-2-methyl-6-p-dimethylaminostyryl-4H-pyran) Special (Radiant Dyes GmbH), cover 545–580 nm, 580–610 nm, and 610–660 nm wavelength ranges, respectively. The periscope allows beam alignment and also changes the polarization of the light from vertical to horizontal. The dye laser output contains a spurious fluorescent background which is filtered with short pass ("3rd Millennium filters" for 580 and 610 nm from Omega Optical Inc.) and band pass ("RazorEdge" for 568, 633, and 647 nm from Semrock Inc.) filters.[13] The light is directed toward the sample with a broadband beam splitter plate (Edmund Optics Inc., NT47-240) with 30% reflection and 70% transmission. A single, long pass interference edge filter ("RazorEdge" for 568, 633, and 647 nm from Semrock Inc.) performs stray light
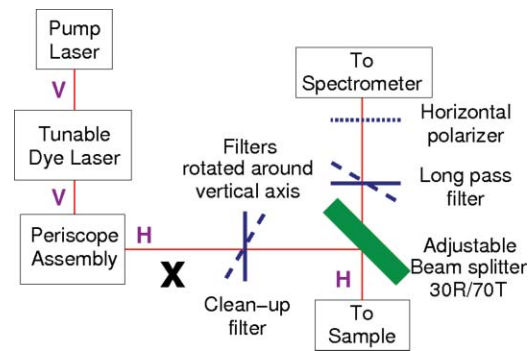

FIG. 1. (Color online) Block diagram of the broadband configuration of the LabRAM spectrometer. V and H denote vertical and horizontal polarizations, respectively. The tunable source is a dye laser pumped with a 532 nm solid state laser. The laser light is aligned with the spectrometer using the periscope element, which also rotates the polarization from vertical to horizontal. The dye laser output is cleaned with a filter. The sample emits a nominally horizontally polarized light, which is the *P* polarization for the long pass filter and the unwanted *S* polarization (vertical) is filtered with the horizontal polarizer. "X" marks where the description is continued in the more detailed Fig. 3.

rejection near the laser excitation and allows operation down to $70-140 \, \text{cm}^{-1}$.

The ability to shift the transmission of the interference filters by rotating them enables broadband operation. In Fig. 2, we show the filter behavior at different incidence angles for a 633 nm long pass filter. The edge of transmission blue shifts upon rotation with respect to normal incidence. However, the shift is smaller for the *S* than for the *P* polarization; i.e., the shift is larger for the horizontally polarized light when the filter is rotated around a vertical axis, such as it is realized in our instrument.

For the *P* polarization, the blue shift upon rotation is $\lambda(\theta) = \lambda_0 \sqrt{1 - (\sin^2 \theta / n^2)}$, where λ_0 is the passband wavelength at normal incidence, n is the effective index of refraction for the filter, and θ is the angle of incidence. For filters with 1 in. apertures (such as the short pass and long pass filters), rotation angles up to 30° were used which yields
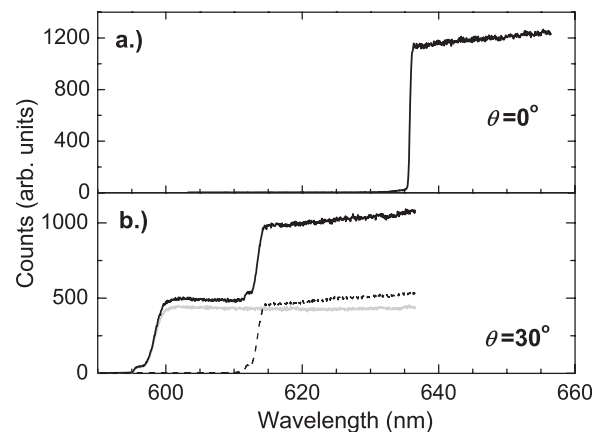

FIG. 2. Transmittance of the 633 nm long pass filter using unpolarized white light; (a) at normal incidence and (b) rotated by 30°. When polarization filters are used, the two parts of the double step feature (solid black line) are separated according to the *S*- and *P*-polarization (dashed black and solid gray lines, respectively). Note the broadening of filter transition width upon rotation.

a blue shift of about 10%. The band pass "Razor edge" filters had an aperture of 0.5 in. which limited the blue shift to about 5%.

The filter transition width broadens for larger incidence angles. This is defined as the maximum difference between the laser wavelength at which the attenuation exceeds optical density 6 and the filter edge wavelength at the 50% transmission point. For the 30° incidence, a fivefold increase in the transition width is observed when compared to the normal incidence. For the "RazorEdge" filters, the $0.2\% \times \lambda$ transition width at normal incidence broadens to $1\% \times \lambda \approx 150 \, cm^{-1}$, which makes it usable for Raman shifts above $\sim 150 \, cm^{-1}$. The less shifted S (in our construction vertically) polarized stray light is removed with a polarization filter before the spectrometer input.

Figure 3 shows the setup for the modified LabRAM spectrometer. For the original spectrometer, the long pass filter mirrors the light toward the sample and also acts as a Rayleigh filter. In our construction, the beam splitter mirrors the light toward the sample and the stray light is filtered with the separate long pass filter, therefore the double function for the filter is split. The broadband beam splitter plate has 30% reflection and 70% transmission, thus only a small fraction of the Raman light is lost. The 70% excitation power loss on the beam splitter can be compensated by reducing the attenuation of the intensive laser beam, maintaining a constant irradiation density on the sample. The beam splitter plate is mounted on a finely adjustable two-axis holder (Thorlabs Inc., VM1) with a home-made mounting. The fine adjustment is required to set the light alignment properly with the spectrometer. Final fine adjustment is performed with the holder to maximize the Raman signal.

The long pass filter is rotated around a vertical axis, which is more practical than rotation around a horizontal one. This preferred axis fixes the optimal light polarization for the whole setup. The vertical rotation axis prefers a horizontally polarized scattered (Raman) light as it is of the P polarization, for which the edge shift is larger. For SWCNTs, the Raman light is polarized preferentially along the polarization of the

excitation, a phenomenon called antenna effect.[9,10] Therefore a horizontally polarized laser excitation is preferred which explains the polarizations used in our design. We also verified that the LabRAM spectrometer itself is not polarization sensitive in contrast to an older triple monochromator system (Dilor XY triple monochromator system) which is about three times more sensitive to the vertical polarization of the scattered light than for the horizontal one.

III. MEASUREMENTS AND DISCUSSION

Measurements were carried out on a HiPCO sample (Carbon Nanotechnologies Inc., Houston, Texas), which was suspended in a 2 wt. % Sodium dodecyl benzene sulfonate (SDBS) in water using sonication. We focused on the radial breathing mode (RBM) Raman range located below $400 \, cm^{-1}$, which is commonly studied to characterize the diameter distribution in SWCNTs.[14] Carbon tetrachloride was used for Raman shift correction and Raman intensity normalization such as in Ref. 7. The LabRAM spectrometer allows to change between a macro- and micromode with a mirror. The macromode is fitted with a sample holder for cuvettes that was provided with the spectrometer. The suspended HiPCO sample was placed in a glass cuvette under the objective of the built-in microscope (Olympus LMPlan $50 \times /0.50$, inf./0/NN26.5, yields about $1 \times 1 \, \mu m^2$ spot size) and the CCl_4 reference sample was placed into the macrocuvette holder. This allowed a stable and robust spectral shift calibration and intensity normalization since the macro/micromode change is reproducible and there is no need for further adjustments nor for sample exchange.

Twenty nine Raman spectra were acquired for laser excitation energies between 1.92 eV (648 nm) and 2.27 eV (545 nm) with an energy resolution of about 12 meV ($\sim 100 \, cm^{-1}$). The spectrometer was operated with a 600 grooves/mm grating and a liquid nitrogen cooled CCD with 1024 pixels along the spectral direction, which yields a ~ 1.3 cm^{-1} Raman shift resolution and $\sim 1800 \, cm^{-1}$ spectral range for 600 nm (both are wavelength dependent). Typical laser powers of 1–5 mW were used with no observable heating effects. This is due to the liquid nature of both samples as a bucky-paper HiPCO sample is heated observably for powers above 1 mW.

Typical measurement time of 4 min for the sample and a few seconds for the reference yields an acceptable signal-to-noise ratio of about 300 as it is shown in Fig. 4. The sample and reference measurements followed each other immediately without moving the grating position, which led to an accurate Raman shift measurement. A measurement cycle which consists of changing the dye laser wavelength, rotating of the laser clean-up and the long pass filters to the appropriate positions, shifting the spectrometer grating, nulling the spectrometer, and acquiring the spectra, lasted typically 8 min. Additional time is needed for the filter exchange (a few minutes) and to change the laser dye and to readjust the beam alignment (about 1 h). We note that once the dye laser is set and the light path is properly aligned with the spectrometer, no further realignment is required when the wavelength is
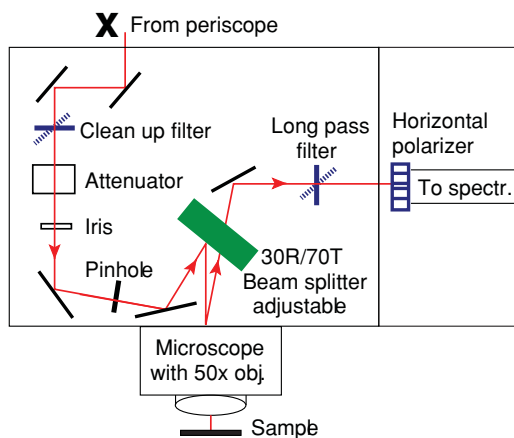

FIG. 3. (Color online) The optical configuration of the modified LabRAM spectrometer including the location for the laser and long pass filters, the beam splitter, and the polarizer. "X" marks the position which is also shown in the block diagram in Fig. 1.
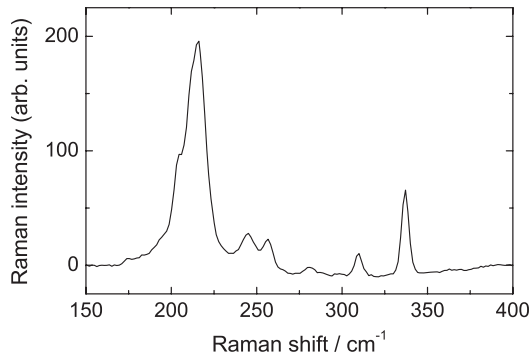
FIG. 4. Raman spectrum of the HiPCO/SDBS suspension for excitation at 592 nm (2.1 eV) with the broadband spectrometer for the RBM range.

FIG. 6. Energy cross section of the Raman map for the RBM of two SWCNTs. The gray squares and black diamonds correspond to cross sections at Raman shifts of 244 and 310 cm^{-1}, respectively. Solid curves refer to the resonance Raman fits as given in the text. Dashed curve shows the calculated resonance Raman profile with a smaller quasiparticle scattering rate, $\Gamma = 10$ meV. The curves are vertically offset for clarity.

changed, even though the filters are rotated and the light is minutely displaced.

In total, 9 h were required to complete the energy dependent Raman experiments with the 29 laser lines including two laser dye exchanges. Measurements of a similar scale such as published previously using a triple monochromator spectrometer[15] last for about 2 weeks, mainly due to the approximately 50 times smaller S/N ratio and the need for a spectrometer realignment upon wavelength change.

Raman shift correction, intensity normalization, and the Raman map preparation was performed using a home-made software. Linear baseline correction was sufficient since no fluorescent response was encountered. Raman shift was corrected for with the carbon-tetrachloride Raman modes at 218 and 314 cm^{-1}. Intensity normalization using CCl_4 is required as it accounts for instrumental uncertainties such as a slight misalignment of the scattered light upon dye exchange. We checked the consistency of the normalization by measuring the same wavelength with different laser dyes after spectrometer realignment.

Figure 5 shows the 2D contour plot of the Raman map. The normalized Raman intensity is displayed on a logarithmic

scale. A good agreement is observed between our data and the measurements in Ref. 7, whose resonance transition energies and Raman shifts are shown for the different SWCNT chiral indexes, (n, m), with full circles. We do not observe the (8,4) SWCNT in our measurement. Points corresponding to the same SWCNT families, i.e., when $2n + m$ is constant[14] are connected by solid lines.

The agreement shows the utility of the broadband arrangement with a clear advantage over previous results in terms of acquisition time. Vertical, i.e., energy cross section of the Raman map were obtained by averaging around a given Raman shift. Representative energy cross section data are shown in Fig. 6, along with fits using the resonance Raman theory[7, 15]

$$I(E_l) \propto \left| \frac{1}{(E_l - E_{22} - i\Gamma)(E_l \pm E_{ph} - E_{22} - i\Gamma)} \right|^2, \quad (1)$$

where $I(E_l)$ is the laser energy (E_l) dependent Raman scattering intensity, Γ is the quasiparticle scattering rate, E_{22} is the transition energy, E_{ph} is the phonon energy.

Fits yield transition energies and quasiparticle scattering rates of $E_{22} = 2.199(1)$ eV and $\Gamma = 71(2)$ meV for the (11,2) SWCNT with $\nu_{RBM} = 244$ cm^{-1}, and $E_{22} = 2.169$ (2) eV and $\Gamma = 59(3)$ meV for the (6,5) SWCNT with $\nu_{RBM} = 310$ cm^{-1}. These values agree well with typical literature values when it is taken into account that the different solvent environment slightly modifies the Raman transition energies.[7]

We note that no further corrections were made to obtain the energy cross section data apart from the normalization by the reference. The result is therefore remarkably smooth in comparison with similar data published in Refs. 7, 12, and 16. This is due to the robust and reproducible measurement of the reference sample and possibility of measuring Raman spectra at different wavelengths without spectrometer readjustment in between.
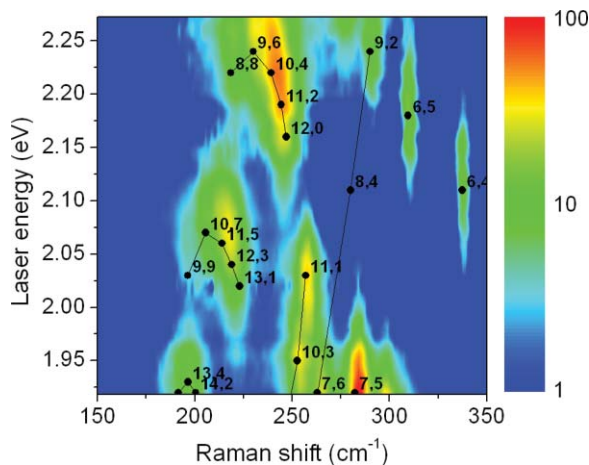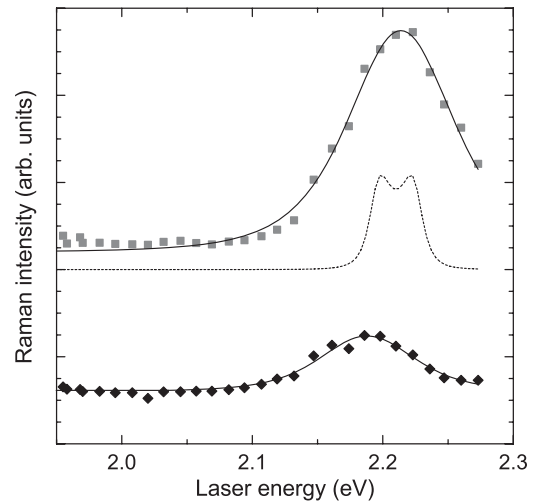

FIG. 5. (Color online) Raman map of HiPCO/SDBS suspension measured with the broadband Raman setup. Logarithmic scale shows the Raman intensity normalized to the maximum observed intensity. Full circles denote data published in Ref. 7.

IV. CONCLUSIONS

In conclusion, we presented the broadband modification of a high sensitivity commercial Raman spectrometer. The improvement allows the use of a tunable dye laser. The spectrometer performance is demonstrated on SWCNTs where such tunable measurements are inevitable to obtain meaningful insights into the vibrational and electronic properties.

ACKNOWLEDGMENTS

[1] M. S. Dresselhaus, G. Dresselhaus, R. Saito, and A. Jorio, Phys. Rep. **409**(2), 47 (2005).
[2] P. R. Carey, Q. Rev. Biophys. **11**(3), 309 (1978).
[3] S. V. Gotoshia and L. V. Gotoshia, J. Phys. D **41**(11), 115406, (2008).
[4] R. M. Martin and L. M. Falicov, *Resonance Raman Scattering* (Springer-Verlag, Berlin, 1983), p. 79.
[5] M. Paillet, F. Meunier, M. Verhaegen, S. Blais-Ouellette, and R. Martel, Rev. Sci. Instrum. **81**(5), (2010).
[6] A. M. Rao, E. Richter, S. Bandow, B. Chase, P. C. Eklund, K. A. Williams, S. Fang, K. R. Subbaswamy, M. Menon, A. Thess, R. E. Smalley, G. Dresselhaus, and M. S. Dresselhaus, Science **275**(5297), 187 (1997).
[7] C. Fantini, A. Jorio, M. Souza, M. S. Strano, M. S. Dresselhaus, and M. A. Pimenta, Phys. Rev. Lett. **93**, 147406 (2004).
[8] The *S* and *P* refer to polarizations which are perpendicular and parallel to the plane of incidence, respectively.
[9] H. D. Sun, Z. K. Tang, J. Chen, and G. Li, Solid State Commun. **109**(6), 365 (1999).
[10] A. Jorio, G. Dresselhaus, M. S. Dresselhaus, M. Souza, M. S. S. Dantas, M. A. Pimenta, A. M. Rao, R. Saito, C. Liu, and H. M. Cheng, Phys. Rev. Lett. **85**, 2617 (2000).
[11] H. Kuzmany, W. Plank, M. Hulman, C. Kramberger, A. Grüneis, T. Pichler, H. Peterlik, H. Kataura, and Y. Achiba, Eur. Phys. J. B **22**(3), 307 (2001).
[12] H. Telg, J. Maultzsch, S. Reich, F. Hennrich, and C. Thomsen, Phys. Rev. Lett. **93**, 177401 (2004).
[13] The use of a short pass filter for laser clean-up limits operation for the Stokes Raman range.
[14] R. Saito, G. Dresselhaus, and M. S. Dresselhaus. *Physical Properties of Carbon Nanotubes* (Imperial College Press, London, 1998).
[15] F. Simon, R. Pfeiffer, and H. Kuzmany, Phys. Rev. B **74**, 212411(R) (2006).
[16] S. K. Doorn, P. T. Araujo, K. Hata, and A. Jorio, Phys. Rev. B **78**(16), 165408 (2008).